STUDY OF THERMAL AND GASDYNAMIC CHARACTERISTICS OF A SUBSONIC PLASMA AIR JET

V. L. Sergeev, A. S. Strogii, and V. A. Tsurko

UDC 533.951.7

Results are presented from a numerical analysis and experimental study of the enthalpy and velocity distributions along and across a subsonic plasma air jet.

In using plasma jets for cutting, welding, fusing, and treating high-melting and heat-reflecting materials, with regard to the plasma-chemical processes it is necessary to know the distribution of the basic parameters of the jet over its length and width in order to select optimum operating regimes.

This article addresses the problem of theoretically and experimentally determining the distribution of velocity and enthalpy in an axisymmetrical, optically fine, submerged plasma air jet issuing from the channel of an electric-arc gas heater (EAGH) into the surrounding atmosphere.

Flow of the plasma jet will be described theoretically using the boundary-layer method [1]. The flow is assumed to be steady and laminar, with local thermodynamic equilibrium. No external electrical or magnetic fields are superimposed, gravity forces are negligibly small, and pressure is constant. Effects connected with diffusion and chemical reactions are not considered.

The system of differential equations describing the flow of the plasma jet with allowance for the above assumptions may be written as follows:

energy equation

$$\rho u \frac{\partial h}{\partial x} + \rho v \frac{\partial h}{\partial r} = \frac{1}{r} \frac{\partial}{\partial r} \left(\frac{\mu r}{\mathrm{Pr}} \frac{\partial h}{\partial r} \right) + \mu \left(\frac{\partial u}{\partial r} \right)^2 - \psi; \tag{1}$$

equation of motion

$$\rho u \frac{\partial u}{\partial x} + \rho v \frac{\partial u}{\partial r} = \frac{1}{r} \frac{\partial}{\partial r} \left(\mu r \frac{\partial u}{\partial r} \right); \tag{2}$$

continuity equation

$$\frac{\partial}{\partial x} (\rho u r) + \frac{\partial}{\partial r} (\rho v r) = 0. \tag{3}$$

System (1)-(3) is closed by the equation of state and the enthalpy dependences of the transfer and thermophysical property coefficients.

The boundary conditions allow for smooth joining of the jet with the environment:

$$x = 0,\ 0 \leqslant r \leqslant r_0,\ h = h_0(r),\ u = u_0(r),\ v = 0, \tag{4}$$

$$x > 0,\ r = 0,\ \partial h/\partial r = 0,\ \partial u/\partial r = 0,\ v(x,\ 0) = 0, \tag{5}$$

$$x > 0,\ r = \delta,\ u = 0,\ \partial u/\partial r = 0, \tag{6}$$

$$x > 0,\ r = \Delta,\ h = h_\infty,\ \partial h/\partial r = 0. \tag{7}$$

Instead of the usual equation of state, we used an equation approximating an isobaric connection between density and enthalpy $\rho = Ah^{-n}$ and making it possible to consider dissociation

A. V. Lykov Institute of Heat and Mass Transfer, Academy of Sciences of the Belorussian SSR. Institute of Mathematics, Academy of Sciences of the Belorussian SSR, Minsk. Translated from Inzhenerno-Fizicheskii Zhurnal, Vol. 42, No. 1, pp. 34-39, January, 1982. Original article submitted October 9, 1980.

0022-0841/82/4201-0025$07.50

and ionization of the gas [2]. The dependence of the viscosity of air on enthalpy was approximated with the data in [3], while data from [4] was used for emissivity.

For reducing the equations to dimensionless form, we took the nozzle radius as the characteristic length and parameter values in the center of the cross section at the nozzle edge as the other characteristic values.

The system of differential equations for the plasma jet was solved by the method of finite differences. To find an approximate solution to the problem being examined, we introduced a lattice of points $\omega = \{(r_k, x_n): r_k = k\tau_1,\ k = 0, 1, 2, \ldots K_x,\ K_x\tau_1 = L_x,\ L_{x/x=0} = 1;\ x_n = n\tau_2,\ n = 0, 1, 2, \ldots N,\ N\tau_2 = X\}$ on which the system (1)-(3) is approximated by difference equations [5]:

$$r\rho(y)\,zy_{\bar{x}} + r\rho(y)\,wy_{\overset{\circ}{r}} = C_1(a(y,\ r)\,y_{\bar{r}})_r + C_2 r\mu(y)\,z^2_{\overset{\circ}{r}} + C_3 r\psi(y), \tag{8}$$

$$k = 1,\ 2 \ldots K_x - 1,\quad n = 1,\ 2 \ldots N,$$

$$y_{1,n} - y_{0,n} - \frac{1}{3}\,(y_{2,n} - y_{1,n}) = 0, \tag{9}$$

$$y_{K_x,n} - y_{K_x-1,n} - \frac{1}{3}\,(y_{K_x-1,n} - y_{K_x-2,n}) = 0, \tag{10}$$

$$r\rho(y)\,zz_{\bar{x}} + r\rho(y)\,wz_{\overset{\circ}{r}} = C_4(a(y,\ r)\,z_{\bar{r}})_r\,, \tag{11}$$

$$k = 1,\ 2 \ldots K_x - 1,\quad n = 1,\ 2 \ldots N,$$

$$z_{1,n} - z_{0,n} - \frac{1}{3}\,(z_{2,n} - z_{1,n}) = 0,\quad z_{K_x} = 0, \tag{12}$$

$$r\,(\rho(y)\,z)_{\bar{x}} + (\rho(y)\,wr)_{\bar{r}} = 0,\quad w_0 = 0, \tag{13}$$

$$k = 1,\ 2 \ldots K_x,\quad n = 1,\ 2 \ldots N.$$

Here y, z, and w are approximate values of h, u, and v, respectively, at the point (r_k, x_n); for the function $f = f(r, x)$:

$$f_{\bar{r}} = \frac{f_{k,n} - f_{k-1,n}}{\tau_1}\,;\quad f_r = \frac{f_{k+1,n} - f_{k,n}}{\tau_1}\,;\quad f_{\overset{\circ}{r}} = \frac{f_{k+1,n} - f_{k-1,n}}{2\,\tau_1}\,; \tag{14}$$

$$f_{\bar{x}} = \frac{f_{k,n} - f_{k,n-1}}{\tau_2}\,; \tag{15}$$

$$a(y,\ r) = \frac{1}{2}\,[r_k\mu(y)|_{k,n} - r_{k-1}\mu(y)|_{k-1,n}]; \tag{16}$$

$$C_1 = \frac{1}{\mathrm{Re}_0\,\mathrm{Pr}_0}\,;\quad C_2 = \frac{\mu_0 u_0}{\rho_0 h_0 r_0}\,;\quad C_3 = \frac{\psi_0 r_0}{\rho_0 u_0 h_0}\,;\quad C_4 = \frac{1}{\mathrm{Re}_0}\,; \tag{17}$$

C_1, C_2, C_3, and C_4 are dimensionless complexes obtained in reducing the initial equations to dimensionless form. The above equations are solved by iteration in the following manner

$$r\rho(\overset{s}{y})\,\overset{s}{z}\,\overset{s+1}{y}_{\bar{x}} + r\rho(\overset{s}{y})\,\overset{s}{w}\overset{s}{y}_{\overset{\circ}{r}} = C_1(a(\overset{s}{y},\ r)\,\overset{s+1}{y}_{\bar{r}})_r + C_2 r\mu(\overset{s}{y})\,\overset{s}{z}{}^2_{\overset{\circ}{r}} + C_3 r\psi(\overset{s}{y}), \tag{18}$$

$$k = 1,\ 2 \ldots K_x - 1,\quad n = 1,\ 2 \ldots N,$$

$$\overset{s+1}{y}_{1,n} - \overset{s+1}{y}_{0,n} - \frac{1}{3}\,(\overset{s}{y}_{2,n} - \overset{s}{y}_{1,n}) = 0, \tag{19}$$

$$\overset{s+1}{y}_{K_x,n} - \overset{s+1}{y}_{K_x-1,n} - \frac{1}{3}\,(\overset{s}{y}_{K_x-1,n} - \overset{s}{y}_{K_x-2,n}) = 0, \tag{20}$$

$$r\rho(\overset{s+1}{y})\,\overset{s}{z}\,\overset{s+1}{z}_{\bar{x}} + r\rho(\overset{s+1}{y})\,\overset{s}{w}\overset{s}{z}_{\overset{\circ}{r}} = C_4(a(\overset{s+1}{y},\ r)\,\overset{s+1}{z}_{\bar{r}})_r\,, \tag{21}$$

$$k = 1,\ 2 \ldots K_x - 1,\quad n = 1,\ 2 \ldots N,$$

$$\overset{s+1}{z}_{1,n} - \overset{s+1}{z}_{0,n} - \frac{1}{3}\,(\overset{s}{z}_{2,n} - \overset{s}{z}_{1,n}) = 0,\quad \overset{s+1}{z}_{K_x,n} = 0, \tag{22}$$

$$r(\overset{s+1}{\rho(y)}\ \overset{s+1}{z})_{\bar{x}} + (\overset{s+1}{\rho(y)}\ \overset{s+1}{wr})_{\bar{r}} = 0,\ \overset{s+1}{w}_{0,n} = 0,$$
$$k = 1,\ 2\ \ldots\ K_x,\ n = 1,\ 2\ \ldots\ N,\ s = 0,\ 1,\ 2,\ 3\ \ldots \qquad (23)$$

Calculations are performed with Eqs. (18)-(23) as follows: assuming that the s-th values of all the sought quantities on the n-th layer have been found, we use the known approximate values of y, z, and w on the (n − 1)-th layer and Eq. (18) to find the (s + 1)-th values of y. We then determine $\overset{s+1}{z}$ from (21) and $\overset{s+1}{w}$ from (23). We proceed in a similar manner from the (s + 1)-th approximation to the (s + 2)-th approximation. The iteration procedure is continued until we obtain agreement between two successive approximations with an assigned accuracy ε, i.e., until satisfaction of the inequality

$$\max_k |\overset{s+1}{y}_{k,n} - \overset{s}{y}_{k,n}| < \varepsilon. \qquad (24)$$

The value of ε is chosen in accordance with the number of steps τ_1 and τ_2.

To obtain a submerged high-temperature air jet in the experiments, we used an EAGH with eddy stabilization and self-adjusting arc length. The flow from the plasmatorn nozzle was subsonic. The mass flow rate of the gas was set by means of a pressure regulator installed ahead of the flow nozzle. Gas pressure before the nozzle was read from a standard manometer. The power in the arc was changed without changing the gas flow rate by using a ballast rheostat.

The measurements were made in jets from plasmatrons with electrode diameters of 15 and 20 mm operated in regimes characterized by arc powers of 40, 50, 70, and 120 kW. Gas flow rates were 2.5, 3.5, and 5.5 g/sec. The radial distributions of the parameters were measured in the maximum regime in cross sections 5, 20, 40, and 70 mm from the nozzle edge.

The parameters of the jet were measured with a combination transducer which permitted simultaneous measurement of the change in the heat flow from the jet to a barrier over time and the stagnation pressure in the plasma flow. The method of a semiinfinite body [6] was used to determine the arbitrarily time-varying heat flux. Here, the temperature of a calorimetric element was measured with Chromel—Copel thermocouples embedded 1-2 mm below the surface of a heat exchanger.

To simultaneously measure the stagnation pressure, a hole was drilled in the copper cylinder of the heat-flux transducer. The end of the hole opposite the working end was connected with a strain-gauge pressure transducer. The ratio of the area of the hole to the area of the end of the transducer was 1/100. The transducer permits measurement of pressure change in tenths to hundredths of an atmosphere with frequencies up to 300 Hz. The working frequencies of the heat-flux transducer range up to 100 Hz. The heat fluxes measured by transducers with and without the drilled hole agree satisfactorily [7]. The combination transducer is advanced over a section of the jet by an electric motor. The location of the transducer in the jet is determined by a special coordinate finder. The temperature of the thermocouples, stagnation pressure, and transducer coordinates were recorded over time with an N030A cathode-ray oscillograph. Heat fluxes were calculated on an "Elektronika S50" computer.

The enthalpy of the gas was determined from the steady-state dependence of the heat flux to a spherical body in the vicinity of the stagnation point on the parameters of the gas flow with a laminar flow of equilibrium dissociated air or nitrogen [8]:

$$q = 4.5 \cdot 10^{-4} R^{-0.5} (p - p_\infty)^{0.25} p^{0.25} (h - h_w). \qquad (25)$$

The velocity of the plasma flow was found from measurements of the dynamic head, with allowance for the enthalpy dependence of density.

Figure 1 shows a comparison of the theoretical and experimental radial distributions of the parameters of the plasma air jet. The numerical calculations were performed by the method described above on a BÉSM-6 computer. The experimental dimensionless profiles of enthalpy and velocity agree satisfactorily with the theoretical curves obtained from the solution of Eqs. (1)-(3). The parameter profiles are similar along the jet and are approximated well by Gaussian curves:

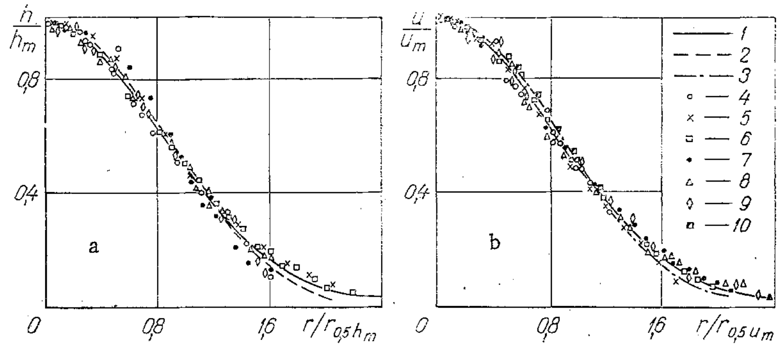

Fig. 1. Profiles of enthalpy (a) and velocity (b) in a plasma air jet. Calculation: 1) with (1)-(3); 2) with (26); 3) with (27). Experiment: 4-7) our data, h_{om} = 47,250 kJ/kg; 4) x/r_o = 0.5; 5) 2; 6) 4; 7) x/r_o = 7; 8) [9], x/r_o = 8.3-16.7, h_{om} = 7680 kJ/kg; 9) [10], x/r_o = 17-43, h_{om} = 6980-10,860 kJ/kg; 10) [14], x/r_o = 0.5, h_{om} = 70,000 kJ/kg.

$$h/h_m = \exp[-\ln 2 (r/r_{0.5\,h_m})^2], \qquad (26)$$

$$u/u_m = \exp[-\ln 2 (r/r_{0.5\,u_m})^2]. \qquad (27)$$

Relations for determining the thermal and dynamic half-widths of the jet were obtained by approximating the numerical results and have the following form:

$$r_{0.5\,h_m}(x) = r_{0.5\,h_{om}} + 0.07\,x, \qquad (28)$$

$$r_{0.5\,u_m}(x) = r_{0.5\,u_{om}} + 0.05\,x. \qquad (29)$$

Also shown in Fig. 1 is experimental data from [9] and [10] on a turbulent plasma air jet. This data shows that the profiles of the parameters of laminar and turbulent jets are similar for the main sections of the jet. The turbulent jet is described formally by the same differential equations as in the case of laminar flow, except for a substitution of transfer coefficients [1].

Enthalpy and velocity decrease more rapidly along the axis in the plasma jet than in a cold jet (Fig. 2) due to the large difference in the densities of the hot and cold gas. Comparison of the distributions of the plasma-jet parameters shows that enthalpy falls more rapidly than velocity along the jet and that the thermal boundary of the jet is broader than the dynamic boundary ($r_{0.5}h_m > r_{0.5}u_m$). This conclusion is consistent with the representations of the theory of jets [11].

The character of change of the axial parameters is affected by the initial distribution of the parameters. As shown by an analysis of experimental and theoretical studies performed in [12], this distribution is close to parabolic. This is explained by the fact that the length of the core of the jet, with constant values of velocity and enthalpy, is relatively small and, in our experiments, did not exceed one gauge.

Comparison of the axial distributions of the parameters of the laminar jet shows satisfactory agreement between the theoretical and experimental results up to gauge eight. With a further increase in distance from the nozzle edge, the measured drop in the parameters is more rapid than the calculated decrease. This is attributable to an increase in the rates of exchange with the environment due to the transition from laminar to turbulent flow. At x/r_o > 14, the experimental data agrees with the results in [9] and [10] for a turbulent jet. The transition of the plasma air flow to the turbulent regime at this distance was noted in [13].

The difference in the numerical results obtained for our conditions with and without allowance for the radiation of the jet did not exceed 8%. Radiation may determine the thermal state of the medium if the pressure is high and there is a high degree of initial heating [16].

Thus, the completed study of the characteristics of a plasma air jet showed that the above-described method of determining the distribution of parameters over the length and

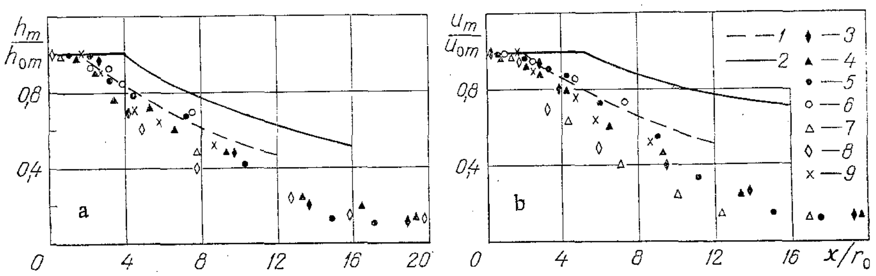

Fig. 2. Axial change in enthalpy (a) and velocity (b) in a plasma air jet. Calculation: 1) with (1)-(3); 2) data from [1] for a cold jet. Experiment: 3-6) our data; 3) h_{om} = 24,500 kJ/kg; u_{om} = 350 m/sec; 4) 27,400 and 370; 5) 43,900 and 410; 6) 47,250 and 640; 7) [9], h_{om} = 7680 kJ/kg; 8) [10] h_{om} = 6980-10,860 kJ/kg; 9) [15], h_{om} = 13,630 kJ/kg; u_{om} = 220 m/sec.

radius of the jet gives results which agree satisfactorily with empirical data and can be used to determine optimum parameters for a laminar jet from an EAGH in different production operations.

NOTATION

x, r, axial and radial coordinates; u, v, axial and radial components of velocity; ρ, density, μ, viscosity; ψ, emissivity; $r_{0.5}$, radius at which local value of velocity or enthalpy is half its axial value; δ, Δ, radii of dynamic and thermal boundary layers; q, heat flux, kW/m^2; h, h_w, stagnation enthalpy and enthalpy at wall temperature, kJ/kg; p, p_∞, stagnation pressure and static pressure, Pa; R, radius of curvature of spherical front part of body. Indices: 0, conditions at nozzle edge; m, conditions on jet axis; ∞, conditions on outer boundary of jet.

LITERATURE CITED

1. G. Schlichting, Boundary Layer Theory, McGraw-Hill.
2. W. L. Bade, "Simple analytical approximation to the equation of state of dissociated air," ARS J., 29, No. 4, 298-299 (1959).
3. N. B. Vargaftik, Tables on the Thermophysical Properties of Liquids and Gases, Halsted Press (1975).
4. V. A. Kamenshchikov, Yu. A. Plastinin, V. M. Nikolaev, and L. A. Novitskii, Radiative Properties of Gases at High Temperatures [in Russian], Mashinostroenie, Moscow (1971).
5. A. A. Samarskii, Theory of Difference Methods [in Russian], Nauka, Moscow (1977).
6. G. T. Aldoshin, A. S. Golosov, and V. I. Zhuk, "Solution of an inverse problem of transient heat conduction," in: Heat and Mass Transfer [in Russian], Vol. 8, Nauka i Tekhnika, Minsk (1968), pp. 186-199.
7. V. L. Sergeev, "Transient heat exchange between a barrier and a gas flow near the stagnation point," in: High-Temperature Heat Exchange and Mass Transfer Under Steady and Unsteady Conditions [in Russian], A. V. Lykov Institute of Heat and Mass Transfer, Academy of Sciences of the Belorussian SSR, Minsk (1978), pp. 140-158.
8. V. L. Sergeev, G. M. Bezladnov, and V. D. Lyashkevich, "Experimental study of the heating of a blunt body by a plasma flow," Inzh.-Fiz. Zh., 20, No. 4, 622-627 (1971).
9. V. Ya. Bezmenov and V. S. Borisov, "Turbulent air jet heated to 4000°K," Izv. Akad. Nauk SSSR, Otd. Tekh. Nauk Energ. Avtom., No. 4, 42-45 (1961).
10. V. F. Sivirkin and N. M. Rogachev, "Study of a turbulent plasma jet," Teplofiz. Vys. Temp., 12, No. 1, 128-136 (1974).
11. I.-Shi-Bai, Theory of Jets [in Russian], Moscow (1960).
12. A. V. Donskoi and V. S. Klubnikin, Electroplasma Processes and Equipment in Machine Construction [in Russian], Mashinostroenie, Leningrad (1979).
13. A. V. Bolotov, D. O. Tobayakov, and L. A. Tonkonogaya, "Experimental study of the gasdynamic characteristics of a laminar plasma jet," in: Sixth All-Union Conference on Low-Temperature-Plasma Generators, Frunze: Ilim (1974), pp. 440-443.
14. F. B. Yurevich and M. V. Volk-Levanovich, "Velocity of a plasma jet," Vestsi Akad. Navuk BSSR Ser. Fiz. Tekh. Navuk, No. 1, 125-128 (1966).

15. A. T. Neklesa and S. P. Polyakov, "Probe measurements of the thermal structure of a plasma air jet," in: Eighth All-Union Conference on Low-Temperature-Plasma Generators, Vol. 1, Institute of Thermal Physics, Siberian Branch, Academy of Sciences of the USSR, Novosibirsk (1980), pp. 221-224.
16. V. P. Zamuraev, S. S. Katsnel'son, G. A. Koval'skaya, I. I. Maslennikova, V. G. Sevast'yanenko, and R. I. Soloukhin, "Radiative heat transfer in a low-temperature plasma," in: Eighth All-Union Conference on Low-Temperature-Plasma Generators, Vol. 1, Institute of Thermal Physics, Siberian Branch, Academy of Sciences of the USSR, Novosibirsk (1980), pp. 109-112.

EFFECT OF THE AERODYNAMIC STRUCTURE OF A FLOW ON THE HYDRAULIC CHARACTERISTICS OF THE DIFFUSER OF A FLAT-FLAME INJECTOR TORCH

R. K. Narkhodzhaev and E. R. Kasparov UDC 662.951.23/27:533.6

It is experimentally established that the admission of a twisted flow into a diffuser makes it possible to increase the expansion angle of the flow and reduce the dimensions of the torch.

Conical and plane diffusers with small divergence angles [1-3] are commonly used in various aerodynamic systems in the case of potential flow to smooth out the velocity profile and increase total pressure. Separated flows, arising at angles greater than 5-10°, place limitations on the degree of divergence of the diffuser. Such flows favor the formation of eddies and stagnant zones, which leads to dissipation of the flow energy and pressure loss. The main characteristic of the diffuser is the impact efficiency, which is determined experimentally for different divergence angles. This characteristic is inserted into a formula for determining the pressure loss from the difference in velocities in the inlet and outlet sections of the diffuser [2, 3]

$$\Delta P = \frac{(w_1 - w_2)^2}{2g}\,\varphi_{\mathrm{dif}}. \tag{1}$$

The problem posed here was to obtain a flat flame 300 mm wide at the combustion front using a cylindrical mixing chamber 50 mm in diameter and having a minimum distance between the inlet and outlet sections of the diffuser. The chamber was chosen on the basis of the capacity of the torch, while the width of the flame was chosen on the basis of processing considerations connected with the area of application of the torch. The losses in the diffuser were limited by the excess gas pressure of 50 kPa and flow rate of 1 m^3/h (the maximum permissible quantity of vapor phase of the liquified gas taken from the 50-liter container).

The above problem cannot be solved with a diffuser with the recommended divergence angle of 5° [3], since the above dimensions for the mixing chamber and outlet section would give the diffuser a length of several dozen gauges. This would in turn increase friction losses of the kinetic energy of the flow and the dimensions of the torch.

A broad flame front could be obtained only by introducing a twisted flow into the diffuser cavity. It was suggested a priori that the more intensive development of such a flow [4] would ensure unseparated flow in a diffuser with a large divergence angle. Three diffusers with divergence angles of 45, 60, and 75° and curvilinear generatrices were studied on the basis of this proposal. The inlet sections of the diffusers were made circular, with a diameter equal to the diameter of the mixing chamber. The circle was made into an ellipse going away from the inlet, with the ellipse degenerating into a slit with the dimensions 300 × 6 mm at the diffuser outlet [5]. This optimum shape for the diffusers was chosen in accordance with the work [6], where the authors give preference to diffusers with a convex inlet section and a rectilinear continuation to a concave outlet section.

Mid-Asiatic Affiliate of the All-Union Scientific-Research Institute of Gas Utilization in the National Economy and of Underground Storage of Petroleum, Petroleum Products, and Liquified Gas (VNIIpromgaz). Translated from Inzhenerno-Fizicheskii Zhurnal, Vol. 42, No. 1, pp. 40-42, January, 1982. Original article submitted September 16, 1980.

 0022-0841/82/4201-0030$07.50